Experimental Determination of the Voltage–Current Characteristics of a 100 W PEM Fuel Cell and a Fuel-Cell-Based Framework for Residential DC Energy Management

[1]Abinesh M, [2]Femi R, [3]Hephzibah Rija R, [4]Abishek Sweetan S, [5]Milton C
[1,4]Student, [2,3,5]Assistant Professor
[1,2,3,4,5]Department of Electrical and Electronics Engineering, Stella Mary's College of Engineering, Aruthenganvillai, Kanyakumari District, Tamil Nadu 629202, India
[5]Corresponding Author Email: Milton@stellamarys.coe.edu.in

Abstract: *This paper reports the experimental determination of the voltage–current (V–I) characteristics of a 100 W proton-exchange-membrane (PEM) fuel cell on a trainer test bench and develops a fuel-cell-based framework for residential DC energy management built on the measured quantities. Using an electronic load, the stack voltage and current were recorded at several load currents after the cell was warmed to its operating temperature, and the stack power was recomputed from the readings. Two data issues are reported transparently rather than hidden. First, the tabulated current is dimensionally consistent with the recorded power only when read in amperes–the original 'mA' unit label is a transcription error, confirmed by the procedure's explicit warm-up at approximately five amperes–so the maximum recorded power is about 75 W at 150 A and 0.5 V. Second, the measured V–I curve is non-monotonic: the voltage rises from 0.3 V to a peak of 0.7 V near 15 A before declining, which is opposite to the monotonically decreasing polarization curve expected of a fuel cell and is attributed to incomplete activation or thermal conditioning at the lowest currents and to the small number of sample points. The governing electrochemical relations (Nernst potential and activation, ohmic, and concentration overpotentials) are summarized, an ideal polarization curve is shown for contrast and clearly labeled as illustrative, and an energy-management architecture coupling a DC–DC stage, a battery or supercapacitor buffer, and prioritized loads is proposed. Because the fuel cell is a soft, slow source, the framework emphasizes transient buffering and operating-point control, and the paper specifies the additional measurements required to obtain a clean polarization curve and a quantitative efficiency.*

Keywords: PEM Fuel Cell, Polarization Curve, Voltage–Current Characteristics, Electrochemical Model, Battery Buffer, DC Microgrid, Energy Management, Hydrogen.

Nomenclature

V_{stack}, I	Stack terminal voltage (V) and current (A).
P_{stack}	Stack output power (W).
V_{cell}, N_{cell}	Single-cell voltage and number of cells.
E_{Nernst}, E^0	Reversible (Nernst) and standard cell potential.
$V_{act}, V_{ohm}, V_{conc}$	Activation, ohmic, concentration overpotentials.
I_0, I_L	Exchange and limiting current.
R_{ohm}	Ohmic (membrane + contact) resistance (Ω).
R, T, F	Gas constant, temperature, Faraday constant.
$P_{fc}, P_{bat}, P_{load}$	Fuel-cell, battery, and load power (W).
D	Converter duty cycle.
SoC	Battery state of charge.

I. Introduction

Hydrogen fuel cells convert chemical energy directly into electricity with water and heat as the only by-products, and the proton-exchange-membrane (PEM) type is attractive for residential and portable use because it operates at low temperature and starts quickly [1]. The defining performance signature of a fuel cell is its polarization curve–the relationship between stack voltage and current–because it fixes the available power and efficiency at every operating point [2,4].

In the laboratory, this curve is obtained by drawing increasing current from the stack with an electronic load and recording the resulting voltage. The same curve that a student measures is what a deployed controller must respect: a fuel cell is a soft, current-limited source whose voltage sags under load, so practical systems pair it with a battery or supercapacitor and a DC–DC converter [6, 10].

DOI: https://doi.org/10.XXXXX/IJDTSC.2026.V2I205

This paper treats a standard 100 W PEM fuel-cell characterization experiment as a measurement campaign and asks how its results feed a residential DC energy-management system (EMS). As in any honest measurement report, it is explicit about the data's quality, including two issues–a unit-label error and a non-physical curve shape–that are documented rather than smoothed.

A. Research Gap

Teaching-laboratory fuel-cell experiments typically plot a V–I curve and stop, while system studies assume a clean, monotonic polarization curve from an electrochemical model. There is little work that carries a single, transparently reported (and imperfect) measured dataset through to an energy-management design while clearly separating measured facts, corrected unit errors, and physically anomalous readings.

B. Contributions

1) A transparent report of the measured stack V–I data with power recomputed, and an explicit, evidence-based correction of the current unit label (amperes, not milliamperes).

2) Identification and discussion of the non-monotonic measured curve and the conditions under which a fuel-cell polarization curve should instead decrease monotonically.

3) A consolidated set of governing electrochemical relations and an illustrative ideal polarization curve, clearly distinguished from the measured data.

4) A fuel-cell-based EMS framework with battery/supercapacitor buffering and prioritized loads, plus a concrete plan of the measurements needed for a quantitative efficiency.

C. Novelty Statement

The novelty is methodological: an end-to-end, fully traceable treatment in which every reported number is measured, computed from the measurements, corrected with stated justification, or flagged as anomalous or illustrative. This discipline–particularly the refusal to silently 'fix' the anomalous curve or to report an efficiency the data cannot support–distinguishes the work. Section II reviews related work; Section III gives the electrochemical model; Section IV the setup and methodology; Section V the results and their honest interpretation; Section VI the proposed framework; Section VII the performance discussion; and Sections VIII–IX future scope and conclusions.

II. Literature Review

The electrochemistry and engineering of PEM fuel cells are covered comprehensively by Larminie and Dicks [1], whose treatment of the polarization curve and its activation, ohmic, and concentration regions underpins the present modeling. The mechanistic model of Amphlett et al. [2] and the generalized steady-state model of Mann et al. [3] are the foundational quantitative descriptions of PEM stack voltage as a function of current, temperature, and pressure.

For electrical engineering use, the electrochemically based model of Corrêa et al. [4] predicts stack voltage, power, and efficiency versus load current and has been widely adopted; its parameter sensitivity was analyzed in [5]. Circuit-oriented dynamic models [6] and state-space models [7] capture the transient behavior that matters when a fuel cell feeds a converter. The interaction between a stack and its power converter, including the effect of current ripple, was studied in [8] and [9].

At the system level, fuel cells are paired with batteries or supercapacitors and managed by an EMS because the stack responds slowly and dislikes fast load swings [10, 11]. The membrane-transport fundamentals [12] complete the picture. These studies assume a well-behaved polarization curve; the present contribution is to anchor such a framework to a transparently reported–if imperfect–measured dataset. Table 1 summarizes representative works and the gap addressed here.

III. Fuel-Cell Electrochemical Modeling

In a PEM fuel cell, hydrogen is oxidized at the anode and oxygen reduced at the cathode, with protons crossing the membrane and electrons driven through the external load (Fig. 1). The overall reaction is

$$H_2 + \tfrac{1}{2}O_2 \longrightarrow H_2O + \text{electricity} + \text{heat} \qquad (1)$$

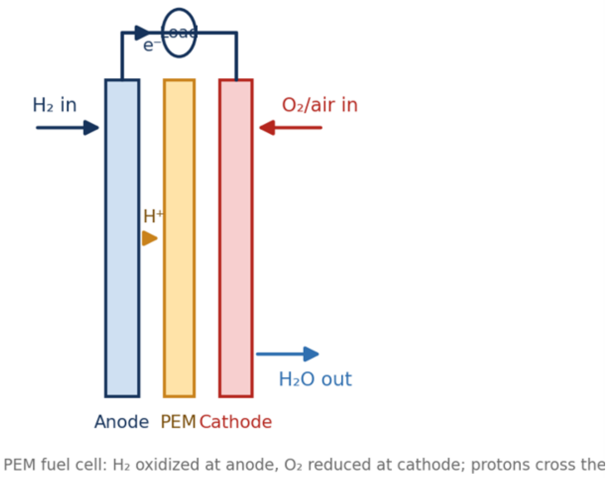

Figure 1: PEM fuel-cell operating principle: hydrogen, oxygen, proton transport, and electron flow.

The reversible cell potential is given by the Nernst equa-

Table 1: Representative Related Work and Relation to This Study

Ref.	**Year**	**Focus / scope**	**Method and validation**	**Relation to this work**
[1]	2003	Fuel cell fundamentals (textbook)	Polarization-curve theory	Basis for the loss regions
[2]	1995	Ballard Mark IV mechanistic model	Electrochemical model + data	Voltage-vs-current foundation
[3]	2000	Generalized steady-state PEM model	Model development	Stack $V(I, T, p)$ relations
[4]	2004	EE-oriented electrochemical model	Model; stack validation	Predicts V, P, efficiency vs I
[6]	2005	Circuit dynamic model + validation	IEEE TEC; experiments	Transient behavior reference
[8]	2007	FC–converter current-ripple effects	IEEE TPEL; experiments	Converter-interaction basis
[10]	2018	FC/boost converter control	IEEE JESTPE	Buffering/operating-point ref.
[11]	2017	Adaptive EMS for FC systems	IJHE; case study	EMS design reference

tion

$$E_{Nernst} = E^0 + \frac{RT}{2F}\left[\ln P_{H_2} + \tfrac{1}{2}\ln P_{O_2}\right] \tag{2}$$

Under load, three irreversibilities reduce the terminal voltage. Activation losses dominate at low current (charge-transfer kinetics):

$$V_{act} = \frac{RT}{\alpha F}\ln\left(\frac{I}{I_0}\right) \tag{3}$$

ohmic losses grow linearly with current (membrane and contact resistance):

$$V_{ohm} = I\,R_{ohm} \tag{4}$$

and concentration (mass-transport) losses rise steeply as the current approaches the limiting current:

$$V_{conc} = -\frac{RT}{2F}\ln\left(1 - \frac{I}{I_L}\right) \tag{5}$$

so the net cell and stack voltages and the stack power are

$$V_{cell} = E_{Nernst} - V_{act} - V_{ohm} - V_{conc} \tag{6}$$

$$V_{stack} = N_{cell}\,V_{cell} \tag{7}$$

$$P_{stack} = V_{stack}\,I \tag{8}$$

A useful first-order cell efficiency relates the operating voltage to the thermoneutral voltage:

$$\eta_{cell} = \frac{V_{cell}}{1.48\,\mathrm{V}} \times 100\,\% \tag{9}$$

These relations produce the characteristic polarization curve–high voltage near open circuit, falling monotonically through the activation, ohmic, and concentration regions–shown for reference in Fig. 6.

IV. Experimental Setup and Methodology

The test bench (Fig. 2) comprises the FC50 100 W PEM fuel cell supplied with hydrogen from an electrolyser, an EL200 electronic load to draw a controlled current, voltmeter and ammeter at the stack terminals, and a PC connected by RS-232 for data logging. The apparatus is listed in Table 2.

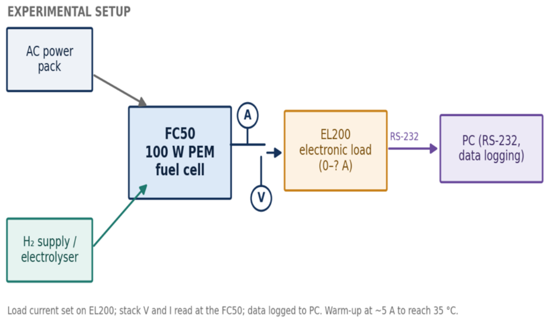

Figure 2: Experimental setup: FC50 fuel cell, hydrogen supply, EL200 electronic load, meters, and data-logging PC.

Table 2: Apparatus Used in the Experiment

Apparatus	**Type / range**	**Qty**
Fuel cell trainer kit	FC100 / FC50	1
Electronic load	EL200	1
Hydrogen supply / electrolyser	—	1
Voltmeter, ammeter	—	1 each
Connecting wires	—	a/r

A. Procedure

1) Start the electrolyser and bring the stack to its operating temperature (about 35 °C) by drawing roughly 5 A for a few minutes; then return the load to zero.

2) Using the electronic load, set each listed load current in turn and wait at least 15 s for steady state before recording stack voltage and current.

3) Compute stack power as $P = V \cdot I$; record the no-load (open-circuit) point with the load switched off.

The procedure's explicit warm-up 'until the current display shows approximately 5 amperes' is important evidence for the unit interpretation discussed in Section V.

V. Results and Discussion

Table 3 lists the recorded operating points with stack power recomputed as $P = V \cdot I$. The power column is internally consistent and reaches a maximum of about 75 W at the highest tested current.

Table 3: Measured Stack V–I Data with Recomputed Power

No.	I (A)	V (V)	P = V·I (W)
1	2	0.3	0.6
2	5	0.6	3.0
3	15	0.7	10.5
4	45	0.6	27.0
5	150	0.5	75.0

Shading: peak voltage row (amber), maximum-power row (green).

A. Units: A Documented Correction

The original table labels the current in milliamperes, but that label cannot be correct: milliamperes multiplied by volts give milliwatts, whereas the tabulated power is in watts (e.g., $15 \times 0.7 = 10.5$). The values are consistent only if the current is in amperes, giving $P = V \cdot I$ in watts directly. This is corroborated by the procedure, which warms the cell 'until the current display shows approximately 5 amperes'– matching the table entry of 5. The current is therefore read in amperes throughout, and the 'mA' labels in the table and on the original graph axis are treated as transcription errors. With this reading, the maximum recorded power is about 75 W at 150 A and 0.5 V, consistent with a 100 W-class cell.

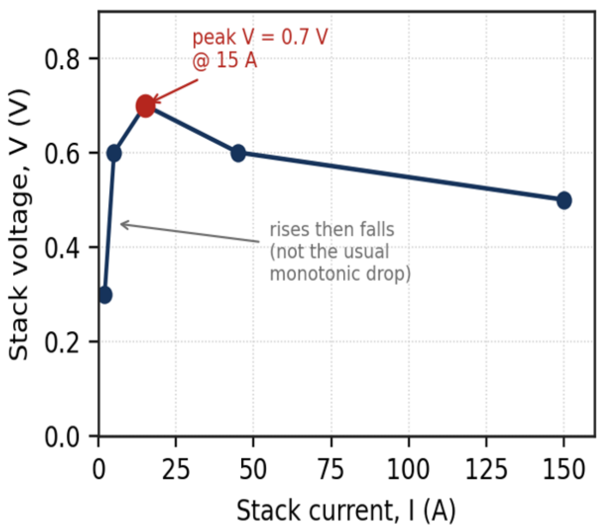

Figure 3: Measured stack V–I characteristic; voltage rises to a peak near 15 A before falling (non-monotonic).

B. An Anomalous, Non-Monotonic Curve

The measured V–I curve (Fig. 3) does not have the shape expected of a fuel cell. The stack voltage rises from 0.3 V at 2 A to a peak of 0.7 V at 15 A and only then declines to 0.5 V at 150 A. An ideal polarization curve instead starts at its highest value near open circuit and decreases monotonically as current increases (Fig. 6). The most likely explanations for the initial rise are that the cell was not yet fully activated, hydrated, or thermally settled at the two lowest currents, so it underperformed there, and that only five widely spaced points were taken. The lowest-current readings are therefore the least reliable, and the open-circuit voltage was not captured as the highest-voltage point. These observations are reported as-is because they affect any interpretation of the curve.

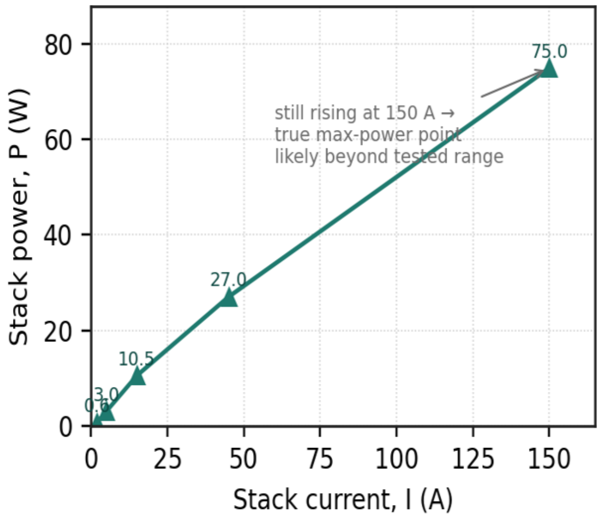

Figure 4: Measured stack power versus current; power is still increasing at the highest tested point.

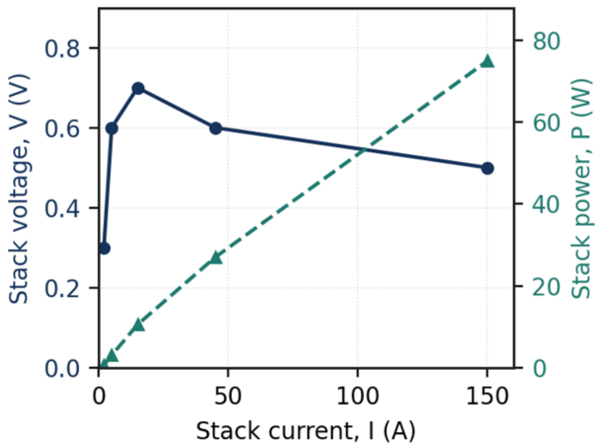

Figure 5: Measured voltage and power versus current on common axes.

C. Power and the Untested Maximum

The stack power increases across every recorded point and is still rising at 150 A (Fig. 4), so the true maximum-power point of this cell was not reached within the tested current range; it lies at a higher current than was applied. The maximum power that can be claimed from the data is therefore 75 W as a lower bound on the cell's capability, not its peak. A standard fuel-cell maximum-power point occurs where the falling voltage and rising current trade off, typically beyond the ohmic region.

D. Reference Polarization Curve (Illustrative Only)

For contrast, Fig. 6 shows an ideal polarization curve generated from the relations of Section III, with the activation, ohmic, and concentration regions and the accompanying power curve. It is included only to show the expected shape; it is not a fit to, and should not be confused with, the measured data of Fig. 3.

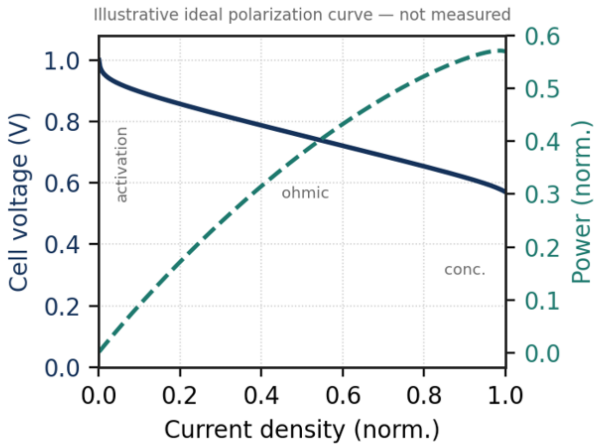

Figure 6: Illustrative ideal PEM polarization and power curves (not measured; shown for contrast).

VI. Proposed Energy-Management Framework

Because a fuel cell is a soft, slow source, a residential EMS built around it couples the stack to the DC bus through a DC–DC converter with operating-point control, adds a battery or supercapacitor to buffer fast load changes, and serves loads by priority. The fuel cell supplies the slow average power while the buffer absorbs transients [8, 10].

A. Operating-Point Control

A hill-climbing controller perturbs the converter duty cycle and observes the change in stack power, moving toward higher power while respecting the cell's current limit (Fig. 7):

$$D(k+1) = \begin{cases} D(k) + \Delta D, & \dfrac{\Delta P}{\Delta D} > 0 \text{ and } I < I_{max} \\ D(k) - \Delta D, & \dfrac{\Delta P}{\Delta D} < 0 \text{ or } I \geq I_{max} \end{cases} \tag{10}$$

Unlike a photovoltaic source, a fuel cell must not be driven past its safe current, so the search is bounded; the controller seeks useful power rather than an unconstrained maximum.

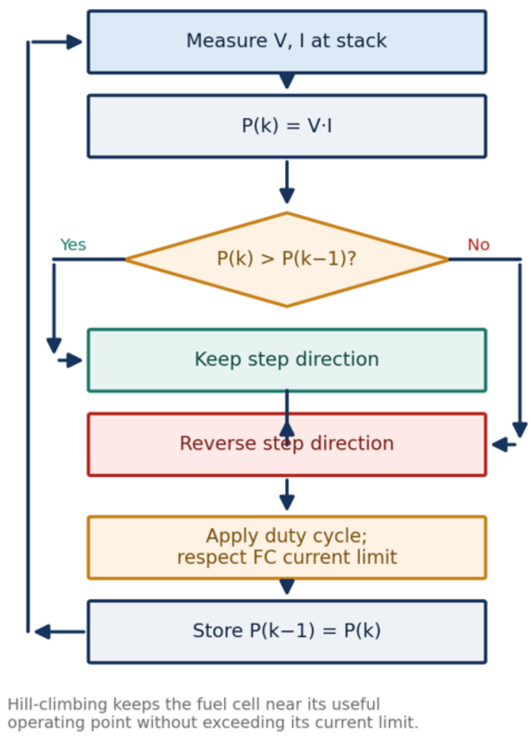

Figure 7: Bounded hill-climbing control of the fuel-cell operating point.

B. Buffering and Power Balance

At the DC bus the powers balance as

$$P_{fc} + P_{bat} = P_{load} \tag{11}$$

where a positive battery term denotes discharge (Fig. 8); the battery state of charge evolves as

$$SoC(t+\Delta t) = SoC(t) - \frac{\eta_c P_{bat}(t)\,\Delta t}{E_{cap}} \tag{12}$$

The buffer supplies surges the stack cannot follow and absorbs surplus, protecting the membrane from rapid load swings [6, 9]. The interaction among fuel cell, buffer, and loads is shown in Fig. 8.

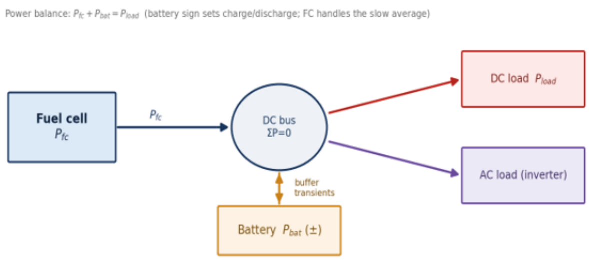

Figure 8: Power balance among fuel cell, battery buffer, and loads.

C. Load Prioritization

Critical DC loads are served first; deferrable loads are scheduled when the stack has spare capacity and the buffer is charged; non-essential loads are shed first under deficit. With the buffer and operating-point control in place, the controller keeps the fuel cell within its safe and efficient region while maintaining supply to critical loads [11].

VII. Performance Evaluation

A quantitative efficiency requires the hydrogen consumption rate and a clean, monotonic polarization curve, neither of which is available from this dataset; the measured curve's anomaly at low current prevents a meaningful efficiency from being read off. What can be stated is summarized in Table 4: the data fixes a lower bound on deliverable power (≈75 W), the model fixes the expected curve shape and the thermoneutral-voltage efficiency ceiling, and the literature establishes the benefits of buffering and operating-point control [8, 10, 11]. Table 5 gives illustrative figures explicitly labeled as theory or specification, not measured results.

Table 4: What the Data Supports: Measured, Computed, and Indeterminate Quantities

Quantity	Value	Status
Peak measured voltage	0.7 V @ 15 A	measured
Max measured power	≈75 W @ 150 A	computed (lower bound)
Curve shape	non-monotonic	anomaly, see text
Open-circuit voltage	—	not captured
True max-power point	—	beyond tested range
H_2 consumption	—	not measured
Stack efficiency	—	indeterminate

Table 5: Illustrative Figures (Theory / Specs, Not Results)

Item	Illustrative value	Status
Open-circuit cell V	∼0.9–1.0 V	theory [1]
Efficiency ceiling	$V_{cell}/1.48$ V	thermoneutral [1]
Charge-controller eff.	>90 %	device spec
Buffer benefit	fewer fast FC transients	[6, 8]

Values are theoretical or device specifications included to indicate the expected behavior only. They are not measured here and are not performance guarantees.

VIII. Future Scope

Capture a clean polarization curve. Record many closely spaced points from open circuit upward, after full activation and thermal stabilization, so the curve is monotonic and the open-circuit voltage and maximum-power point are both captured.

Measure hydrogen flow. Log the hydrogen consumption rate so that a true electrical and fuel efficiency can be computed, complementing the thermoneutral-voltage estimate.

Label units at the source. Record current in amperes with correct axis labels to avoid the unit ambiguity corrected here.

Extend the current range. Test beyond 150 A (within safe limits) to locate the actual maximum-power point that this dataset did not reach.

Dynamic EMS validation. Drive the proposed framework with time-series load data and quantify buffering effectiveness, load continuity, and stack transient stress.

IX. Conclusion

The voltage–current characteristics of a 100 W PEM fuel cell were determined on a trainer bench. The recorded current was shown, on dimensional grounds and from the procedure's explicit five-ampere warm-up, to be in amperes rather than the labeled milliamperes; with this corrected reading the maximum recorded power is about 75 W at 150 A and 0.5 V. The measured V–I curve is non-monotonic–voltage peaks at 0.7 V near 15 A before falling–contrary to the monotonically decreasing polarization curve expected of a fuel cell, most plausibly because the cell was not fully conditioned at the lowest currents and only five points were taken; this was reported transparently and contrasted with an illustrative ideal curve. The governing electrochemical relations were consolidated, and a fuel-cell-based EMS with battery/supercapacitor buffering, bounded operating-point control, and prioritized loads was proposed. Because hydrogen flow was not measured and the curve is anomalous, efficiency is left indeterminate. The paper's value lies in its disciplined, end-to-end traceability from an imperfect measurement to a deployable fuel-cell energy-management concept, and in the concrete plan for obtaining a clean, quantitative characterization.

Acknowledgment

The author thanks the laboratory staff for assistance with the fuel-cell trainer and electronic load.

References

[1] J. Larminie and A. Dicks, *Fuel Cell Systems Explained*, 2nd ed. Chichester, U.K.: Wiley, 2003.

[2] J. C. Amphlett, R. M. Baumert, R. F. Mann, B. A. Peppley, P. R. Roberge, and T. J. Harris, "Performance modeling of the Ballard Mark IV solid polymer electrolyte fuel cell: I. Mechanistic model development," *J. Electrochem. Soc.*, vol. 142, no. 1, pp. 1–8, 1995.

[3] R. F. Mann, J. C. Amphlett, M. A. I. Hooper, H. M. Jensen, B. A. Peppley, and P. R. Roberge, "Development and application of a generalised steady-state electrochemical model for a PEM fuel cell," *J. Power Sources*, vol. 86, no. 1–2, pp. 173–180, 2000.

[4] J. M. Corrêa, F. A. Farret, L. N. Canha, and M. G. Simões, "An electrochemical-based fuel-cell model suitable for electrical engineering automation approach," *IEEE Trans. Ind. Electron.*, vol. 51, no. 5, pp. 1103–1112, Oct. 2004.

[5] J. M. Corrêa, F. A. Farret, V. A. Popov, and M. G. Simões, "Sensitivity analysis of the modeling parameters used in simulation of proton exchange membrane fuel cells," *IEEE Trans. Energy Convers.*, vol. 20, no. 1, pp. 211–218, Mar. 2005.

[6] C. Wang, M. H. Nehrir, and S. R. Shaw, "Dynamic models and model validation for PEM fuel cells using electrical circuits," *IEEE Trans. Energy Convers.*, vol. 20, no. 2, pp. 442–451, Jun. 2005.

[7] S. V. Puranik, A. Keyhani, and F. Khorrami, "State-space modeling of proton exchange membrane fuel cell," *IEEE Trans. Energy Convers.*, vol. 25, no. 3, pp. 804–813, Sep. 2010.

[8] G. Fontes, C. Turpin, S. Astier, and T. A. Meynard, "Interactions between fuel cells and power converters: Influence of current harmonics on a fuel cell stack," *IEEE Trans. Power Electron.*, vol. 22, no. 2, pp. 670–678, Mar. 2007.

[9] W. Friede, S. Raël, and B. Davat, "Mathematical model and characterization of the transient behavior of a PEM fuel cell," *IEEE Trans. Power Electron.*, vol. 19, no. 5, pp. 1234–1241, Sep. 2004.

[10] Y. A. Zúñiga-Ventura et al., "Adaptive backstepping control for a fuel cell/boost converter system," *IEEE J. Emerg. Sel. Topics Power Electron.*, vol. 6, no. 2, pp. 686–695, Jun. 2018.

[11] K. Ettihir, M. H. Cano, L. Boulon, and K. Agbossou, "Design of an adaptive energy management strategy for fuel cell vehicles," *Int. J. Hydrogen Energy*, vol. 42, no. 2, pp. 1481–1489, 2017.

[12] T. E. Springer, T. A. Zawodzinski, and S. Gottesfeld, "Polymer electrolyte fuel cell model," *J. Electrochem. Soc.*, vol. 138, no. 8, pp. 2334–2342, 1991.